

COHERENT HARMONIC EMISSION OF THE ELETTRA STORAGE RING FREE ELECTRON LASER IN SINGLE PASS CONFIGURATION: A NUMERICAL STUDY FOR DIFFERENT UNDULATOR POLARIZATIONS

F. Curbis*, University of Trieste & Elettra, Basovizza, Trieste, Italy,
 H.P. Freund, Science Applications International Corporation (SAIC),
 G. De Ninno, Elettra, Basovizza, Trieste, Italy.

Abstract

The optical klystron installed on the Elettra storage-ring is normally used as interaction region for an oscillator free-electron laser, but, removing the optical cavity and using an external seed laser, one obtains an effective scheme for single-pass harmonic generation. In this configuration the high-power external laser is synchronized with the electron beam entering the first undulator of the optical klystron. The laser-electron beam interaction produces a spatial partition of electrons in micro-bunches separated by the seed wavelength. The micro-bunching is then exploited in the second undulator to produce coherent light at the harmonics of the seed wavelength. The Elettra radiator is an APPLE type undulator and this allows to explore different configurations of polarization. We present here numerical results obtained using the code Medusa for both planar and helical configurations. We also draw a comparison with predictions of the numerical code Genesis.

INTRODUCTION

Coherent Harmonic Generation (CHG) can be implemented in a storage ring using two undulators as a cascade. The first undulator (called modulator) is tuned at the wavelength of an external high-power laser and the second undulator (called radiator) at a higher harmonic of the seed. Between the undulators there is a region, i.e., dispersive section, with a strong magnetic field, which, in single-pass configuration, converts the energy modulation, occurred in the modulator, in spatial modulation (usually referred as “bunching”). The Elettra storage-ring FEL is presently operating in oscillator configuration [1, 2], but, with minor modification, the optical klystron will be used as interaction region for CHG in single-pass configuration. In the new configuration (see Figure 1) the optical cavity will be removed and a conventional laser will be focused into the modulator and synchronized with the electron beam. The main difference between conventional single-pass seeded FEL and storage-ring harmonic generation is that in the latter case the electron beam is re-circulated and not renewed each pass through the optical klystron. This peculiarity determines the maximum repetition rate for this configuration, because the electrons need few synchrotron damping times (order of ten of milliseconds) to cool down after each interaction with the seed laser. Preliminary sim-

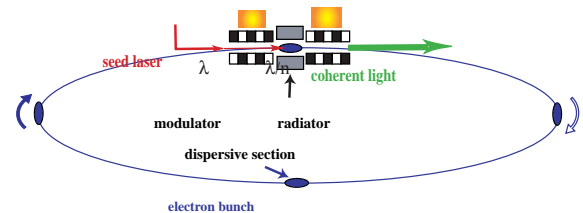


Figure 1: Layout of the Elettra storage-ring FEL after removing the optical cavity and using an external seed laser.

ulations [3] have been done using Genesis [4] for different working points, i.e. different machine (electron-beam energy, Twiss parameters, emittance, strength of the dispersive section) and the seed laser (power and duration) parameters. The work reported in this paper characterizes the emission of the Elettra APPLE-type undulator, operated in both linear and helical configurations. Numerical results are obtained using Medusa and Genesis. Medusa provides the possibility to calculate the harmonic power at the end of the radiator. This means that the radiator is tuned at the third harmonic of the seed laser (i.e. the fundamental in the modulator) and Medusa is able to calculate any desired harmonics besides the fundamental. This will allow to investigate if wavelengths shorter than the fundamental will be detectable. The external seed laser [5] is a titanium-sapphire (Ti:Sa) with a very high peak power (2.5 GW) and very short pulse duration (variable between 100 and 250 fs (RMS)). The repetition rate will be initially 10Hz. Using this frequency, the contribution from incoherent synchrotron emission, provided by electrons circulating in the storage ring but not interacting with the seed laser, may spoil the signal-to-noise ratio. Possible strategies will be explored in the aim of increasing the repetition rate, therefore improving the signal quality. The first undulator is tuned at the fundamental of the seed laser (240 nm), while the second undulator at the third harmonic (80 nm).

OPTIMIZATION FOR MEDUSA SIMULATIONS

In this section we report some studies performed in time-independent mode in order to optimize the parameters before the introduction of the slippage, e.g. time-dependent simulation. The main run parameters used in Medusa simulations are reported in Table 1 [5, 6]. With respect to the

* francesca.curbis@elettra.trieste.it

values used in Genesis simulations, there are some minor differences: the pulse shape of the electron bunch and the seed laser is parabolic instead of Gaussian, the seed duration is 250 fs FWHM instead of 140 fs and the number of periods for both undulators is 22 instead of 20, because Medusa needs one period more at the entrance and exit of the undulator to properly model the simulation. The vari-

Table 1: Run parameters used in Medusa simulations

Electron beam	
Energy	0.9 GeV
Peak current	77 A
x-Emittance	2.46 mm-mrad
y-Emittance	0.246 mm-mrad
Energy-spread	0.12%
Bunch length	27 ps
Bunch charge	1.38 nC
Bunch shape	parabolic
Twiss parameters	
$\alpha_x = 0.24$	$\beta_x = 8.986$
$\alpha_y = 0.89$	$\beta_y = 4.695$ m
Modulator	
Magnitude	5.62 kG
Period	10.0 cm
Length	22 periods
Radiator	
Magnitude	3.00 kG
Period	10.0 cm
Length	22 periods
Undulator-to-undulator gap	0.9 m
Seed laser	
Wavelength	240 nm
Seed power	2.5 GW
Seed duration	0.25 ps
Seed shape	parabolic

ation of the radiator output power versus the dipole field strength in the chicane is shown in Figure 2 for the case of a planar radiator. We have found from Genesis simulation that the energy spread induced by the seed laser is so high that the beam needs only a drift to transform the energy modulation in spatial modulation (bunching). In Medusa simulation instead, the power level when the chicane field vanishes is 1.06 MW (and this is very close to the time-dependent result), but a little more power (about 1.36 MW) could get using a chicane field of about 0.5 kG. However, in order to compare the results of these two codes, we have chosen to set to zero the chicane field also in this case. The same power optimization with respect to the magnetic field has been performed tuning the radiator at the third harmonic (see Figure 3). The output power at 80 nm is about 1.7 MW which is almost a factor two over the value found for the planar undulator. The second harmonic (40 nm) power is not very sensitive to the variation of the chicane

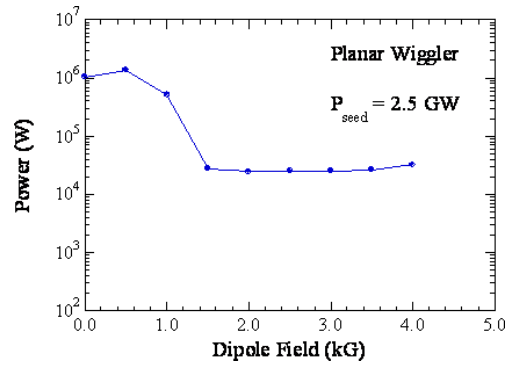


Figure 2: Output power versus dipole field strength at 80 nm for planar radiator.

field and is about 200 W when the chicane field is set to zero. These results have been confirmed by time dependent simulations. The same behavior has been found for a heli-

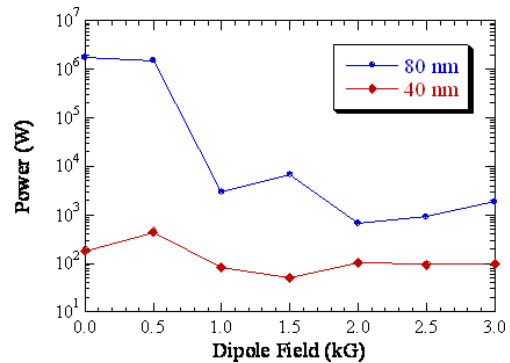


Figure 3: Output power versus dipole field strength for helical undulator tuned at 80 nm and second harmonic (40 nm) power.

cal undulator tuned at the second harmonic (120 nm) of the seed laser. The result, shown in Figure 4, looks similar to previous case: the highest power is found when the chicane field is set to zero and the power is about 4.7 MW at 120 nm and 5.7 kW at 60 nm. As before, while the power at the fundamental (120 nm) drops fast with increasing chicane field, the harmonic power (60 nm) doesn't drop so much. An other important issue to be considered when using numerical codes is the number of simulated particles which is needed in order to guarantee a correct modelization of the process. For the CHG in helical configuration, we found that a larger number of particles is needed with respect to planar configuration. The case for zero energy-spread is reported in Figure 5. We can argue from the results that to do this kind of simulation about 60000 particles per slice are needed without energy spread and, including the energy spread, an order of magnitude more particles is required. In the latter case, the power level will be of course smaller. To conclude, in order to treat the energy spread and the additional harmonics, the following runs used 1210104 particles.

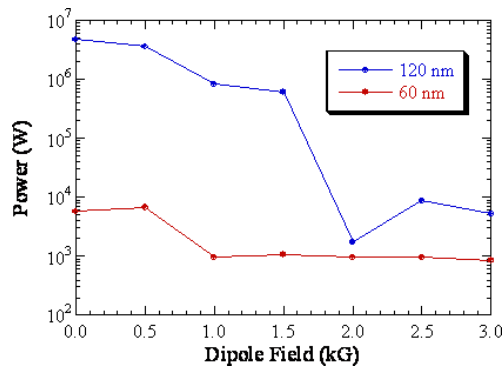


Figure 4: Output power versus dipole field strength for helical undulator tuned at 120 nm and second harmonic (60 nm) power.

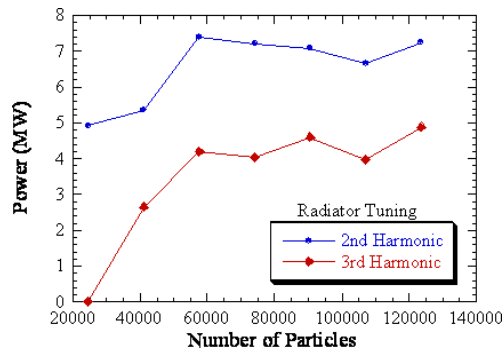


Figure 5: Output power versus number of simulated particles for helical undulator tuned at the second and the third harmonic of 240 nm.

MEDUSA PERFORMANCE

Planar undulator

In time-dependent mode, we firstly looked at the harmonics of the 80 nm wavelength, using 2.5 GW seed power and zero magnetic field inside the dispersive section. The evolution along the undulator of the fundamental (80 nm) and the first three harmonics of that wavelength are shown in Figure 6. The second harmonic (40 nm) reaches a power level of about 2 kW, the third harmonic (26.67 nm) a power level of about 500 W and the fourth harmonic (20 nm) a power of 2 W. While in the steady-state simulations we looked exclusively at the evolution of the power along the radiator, in time-dependent simulations the output temporal profile (see Figure 7) and the harmonic spectrum (see Figure 8) can be displayed. The electron bunch is two order of magnitude longer than the seed laser (27 ps versus 250 fs) and the total slippage, considering 80 nm wavelength and 44-periods undulator, is much smaller than the bunch-length, thus the differences between steady-state and time-dependent simulations are expected to be small. Indeed, the observed peak power is about 1 MW in both cases. The shortness of the laser pulse may lead to numerical problems because one should increase the number of slices

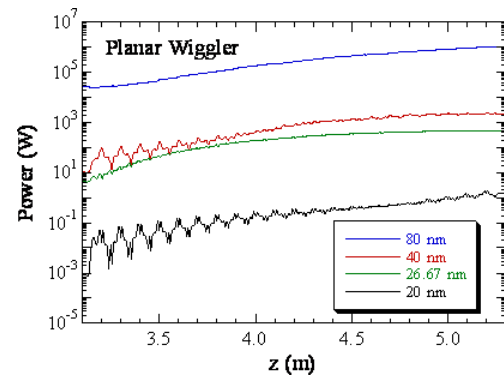


Figure 6: Evolution of the 80 nm radiation and its first three harmonics in planar configuration.

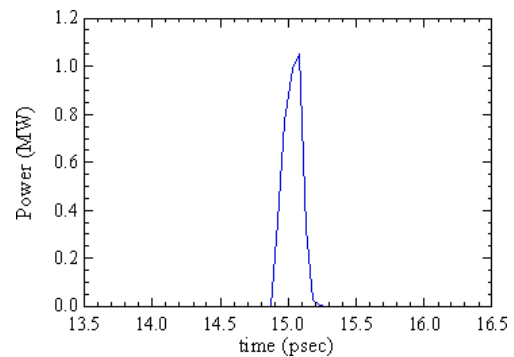


Figure 7: Power versus time of the 80 nm pulse at the end of the radiator in planar configuration.

in order to resolve the FEL pulse structure and an adequate number of particles must be holden in each slice. In our case, the simulation includes 600 slices, with 17496 particles per slice, but only about 10 slices across the seed pulse. This is the reason why the output spectrum in Figure 8 is not smooth and displays a spiky behavior. If one believes the problem is the lack of resolution, the envelope could be considered as the spectral shape. Considering the Fourier

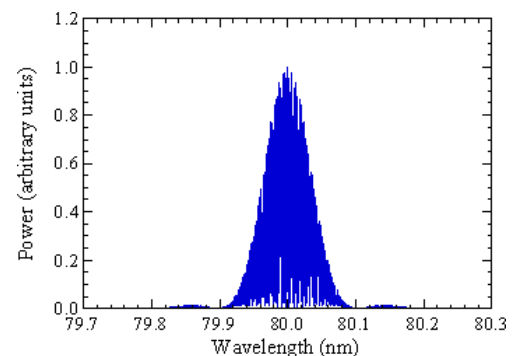


Figure 8: Fourier transform of the output spectrum at 80 nm (planar configuration).

limit, given by the equation:

$$\frac{c \cdot \Delta t [FWHM] \Delta \lambda [FWHM]}{\lambda^2} = 0.441 \quad (1)$$

where c is the speed of light, Δt is the $FWHM$ duration of the output pulse, $\Delta \lambda$ is the $FWHM$ of the output spectrum and λ is the emission wavelength, the results presented here give a quantity that is 1.7 times above the limit. This value indicates that the emitted light have an high level of coherence.

Helical undulator

As already reported before, the steady-state simulation could give enough information about the power level of the 80 nm signal and the first two harmonics of that. For this reason, the simulation of the helical configuration has been obtained in time-independent mode. In Figure 9 the evolution of the signal power along the radiator is displayed. One can observe that the 40 nm harmonic is still about 1 kW as in planar configuration, but the 26.67 nm harmonic has a much lower power than for the planar undulator.

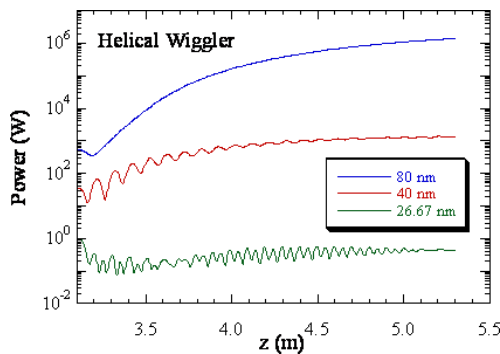


Figure 9: Evolution of the 80 nm radiation and its first two harmonics in helical configuration.

Comparison with Genesis simulation

The campaign of simulation has been completed exploring the helical polarization in Genesis. The power level founded at 80 nm for each configuration is very close between Genesis and Medusa and between planar and helical configuration the differences are lower than one order of magnitude. All Genesis simulation has been performed in time-dependent domain, but, to limit the computing time, just a portion of the electron bunch around the seed pulse has been simulated, with the implicit assumption that the slippage doesn't not affect too much the emission.

The evolution of the output power along the radiator is shown in Figure 10 for both planar and helical configuration. In comparison with Medusa, Genesis results don't exhibit a big difference between planar and helical power. The value found is about 1.1 MW in both cases, as shown also in Figure 11, where the power is plotted as a function of time at the end of the radiator.

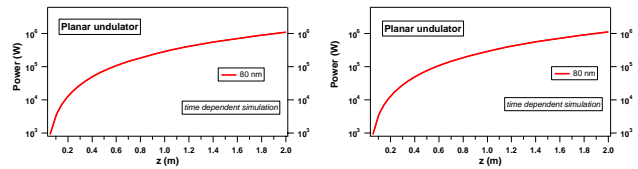


Figure 10: Harmonic power for planar undulator (at left) and helical undulator (at right) obtained tuning the radiator at 80 nm.

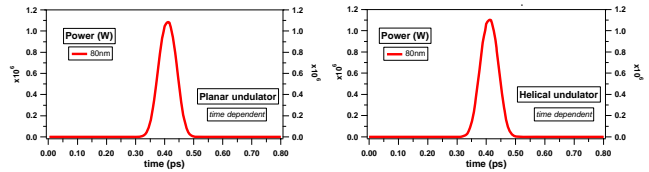


Figure 11: Temporal profile for planar undulator (at left) and helical undulator (at right) obtained tuning the radiator at 80 nm.

The Fourier transform of the output spectrum is reported in Figure 12. Using the Equation 1, we found a value that is 1.6 times above the limit. Also in this case, the radiation emitted shows an high degree of coherence.

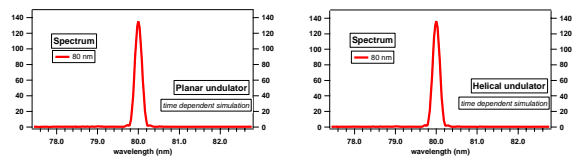


Figure 12: Harmonic spectrum for planar undulator (at left) and helical undulator (at right) obtained tuning the radiator at 80 nm.

CONCLUSION

The Medusa simulations confirmed in general the results already obtained by Genesis, with a good agreement in both planar and helical configuration. Some differences should be longer investigated, i.e., the higher power level found in planar configuration when the dispersive section is 0.5 kG and the factor two more power found in helical radiator.

REFERENCES

- [1] R. P. Walker, Proc. EPAC'99, 93.
- [2] G. De Ninno et al., *Nucl. Instrum. and Meth. A* **483** (2002) 177.
- [3] F. Curbis, G. De Ninno, Proc. FEL'05.
- [4] S. Reiche, *Nucl. Instrum. and Meth. A* **429** (1999) 243.
- [5] M. Danailov, Private Communication.
- [6] F. Iazzourene, Private Communication.